Trinuclear Cluster Complexes Containing the *Furyne* Ligand: Synthesis, Structure, and Properties of the Cycloalkyne Complexes $(CpCo)_n(Cp^*Co)_{3-n}(CO)(\mu_3\text{-}\eta^2\text{-}C_4H_4O)$ (n = 3, 2)

William D. King,[†] Craig E. Barnes,*[,‡] and Jeffery A. Orvis[§]

Departments of Chemistry, University of Tennessee, Knoxville, Tennessee 37996-1600, and Georgia Southern University, Statesboro, Georgia 30460

Received October 11, 1996[⊗]

Cyclopentadienyl-based tricobalt clusters containing the cyclic *furyne* ligand, $\overline{CH_2C{\equiv}CCH_2O}$, have been prepared by the pyrolysis of the butynediol complexes $(CpCo)_3(CO)(RCCR)$, **1**, and $(CpCo)_2(Cp^*Co)(CO)(RCCR)$, **2** (R = CH_2OH). The solid state structures of the furyne complexes, $(CpCo)_3(CO)(\mu_3\text{-}\eta^2\text{-}\overline{CH_2C{\equiv}CCH_2O})$, **3**, and $(CpCo)_2(Cp^*Co)(CO)(\mu_3\text{-}\eta^2\text{-}\overline{CH_2C{\equiv}CCH_2O})$, **4**, verify the presence of the five-membered heterocycle, which formally contains an alkyne group interacting with the tricobalt framework. Chemically and electrochemically reversible one-electron oxidative and reductive couples are observed for **3** at +0.235 and −1.466 V (CH_2Cl_2 solution, Pt electrode, $Fc^{0/+1}$ = +0.482 V), respectively, which are similar to redox features observed for noncyclic analogues. At 171 K, the methylene signals of the furyne ligand in **4** are observed as doublets, indicating that furyne rotation is slow at this temperature. Reversible coalescence of the methylene signals occurs at 195 K, and at room temperature, a single sharp methylene resonance is observed. Total line shape analysis of the coalescing spin system yields the activation parameters for the motion of the furyne ring: $\Delta G^{\ddagger}$ (300 K) = 39.4(2) kJ/mol, $\Delta S^{\ddagger}$ = −18(2) J/mol, and $\Delta H^{\ddagger}$ = 34.0(4) kJ/mol.

Introduction

The ability of transition metals to stabilize metastable organic ligands is one of the more unique themes which have contributed to the development of organometallic chemistry. One subset of this diverse ligand family is the cycloalkynes.[1] Recently, Adams and co-workers have described a family of ruthenium and osmium cluster complexes which contain the cyclobutyne ligand interacting with as many as four metal atoms.[2] These cluster complexes are generally quite stable but can be induced to rearrange with opening of the cyclobutyne ring upon heating. Buchwald *et al.* have prepared a series of reactive zirconocene-based cyclopentyne and cyclohexyne complexes and have described approaches to using these complexes in synthetic schemes involving the stereospecific formation of bicyclic systems.[3] Deeming and co-workers have described several triosmium clusters containing five- and six-membered cycloalkynes,[4] while Wadepohl *et al.* recently reported the synthesis of a number of dihydrido tricobalt cyclopentadienyl clusters containing five-, six-, seven-, and eight-membered cycloalkyne ligands.[5] Bennett and co-workers have recently extended their work on the chemistry of platinum and palladium cyclohexyne complexes to include the first examples involving nickel.[6] Although structural data for these complexes are available, it is difficult to describe in detail the role that the cyclic nature of these strained organic groups may have in influencing the interactions which exist between the metal center(s) and these unique ligands. One reason for this is the lack of suitable model complexes containing noncyclic ligand analogues whose structure, spectroscopy, and reactivity may be compared to the cyclic examples. We have recently described the preparation of a trinuclear cobalt complex containing the *furyne*[7] ligand, $\overline{CH_2C{\equiv}CCH_2O}$.[8] Here, we present a detailed account of the properties of this ligand when bound to a Cp_3Co_3 metal skeleton. Furthermore, via electrochemical measurements, we qualitatively compare the interactions of this ligand with the tricobalt skeleton to those of a noncyclic analogue, the dimethoxybutyne complex.

Results and Discussion

Synthesis and Properties. Heating $(CpCo)_3(CO)$-(RCCR) alkyne complexes (190 °C, 24 h) generally leads

[†] Present address: Department of Chemistry, P.O. Box 1822-B, Vanderbilt University, Nashville, TN 37235.
[‡] University of Tennesee.
[§] Georgia Southern University.
[⊗] Abstract published in *Advance ACS Abstracts,* March 15, 1997.

(1) Bennett, M. A. *Pure Appl. Chem.* **1989**, *61*, 1695.
(2) (a) Adams, R. D.; Chen, G.; Qu, X.; Wu, W.; Yamamota, J. H. *J. Am. Chem. Soc.* **1992**, *114*, 10977. (b) Adams, R. D.; Chen, L.; Qu, X. *Organometallics* **1994**, *13*, 1992.
(3) Buchwald, S. L.; Lum, R. T.; Fisher, R. A.; Davis, W. M. *J. Am. Chem. Soc.* **1989**, *111*, 9113.
(4) (a) Aime, S.; Deeming, A. J. *J. Chem. Soc., Dalton Trans.* **1983**, 1807. (b) Deeming, A. J.; Kabir, S. E.; Powell, N. I.; Bates, P. A.; Hursthouse, M. B. *J. Chem. Soc., Dalton Trans.* **1987**, 1529. (c) Deeming, A. J.; Arce, A. J.; De Sanctis, Y.; Day, M. W.; Hardcastle, K. I. *Organometallics* **1989**, *8*, 1408.
(5) (a) Wadepohl, H. *Comm. Inorg. Chem.* **1994**, *15*, 369. (b) Wadepohl, H.; Gebert, S. H. *Coord. Chem. Rev.* **1995**, *143*, 535.
(6) Bennett, M. A.; Johnson, J. A.; Willis, A. C. *Organometallics* **1996**, *15*, 68.
(7) IUPAC name: 1-oxa-3-cyclopentyne.
(8) Barnes, C. E.; King, W. D.; Orvis, J. A. *J. Am. Chem. Soc.* **1995**, *117*, 1855.
(9) (a) King, R. B.; Harmon, C. A. *Inorg. Chem.* **1976**, *15*, 879. (b) Yamazaki, H.; Wakatsuki, Y.; Aoki, K. *Chem. Lett.* **1979**, 1041. (c) Fritch, J. R.; Vollhardt, K. P. C.; Thompson, M. R.; Day, V. W. *J. Am. Chem. Soc.* **1979**, *101*, 2768. (d) Fritch, J. R.; Vollhardt, K. P. C. *Angew. Chem., Int. Ed. Engl.* **1980**, *19*, 559.

S0276-7333(96)00867-9 CCC: $14.00

Table 1. Spectral Data for Complexes 1−5

compound	^{1}H NMR[a]	^{13}C NMR[b]	ν_{co}[c]	MS[d]
1[f]	4.51 (Cp), 4.81 (d, CH_2), 2.61 (t, OH)	85.8 (Cp),[e] 73.3 (CH_2), 160.2 (C≡C)	1683, 1683^{KBr}	486 (M^+, 14), 468 ($M^+ - H_2O$, 100), 440 ($M^+ - H_2O - CO$, 22)
2	4.57 (Cp), 1.40 (CH_3), 4.83 (d, CH_2), 3.16 (t, OH)	84.46 (Cp), 9.84 (C_5Me_5), 95.79 (C_5Me_5), 72.12 (CH_2), 158.26 (C≡C), 283.56 (CO)	1667	556 (M^+, 100), 538 ($M^+ - H_2O$, 89), 510 ($M^+ - H_2O - CO$, 14)
3	4.44 (Cp), 5.26 (CH_2)	85.05 (Cp), 82.28 (CH_2), 153.53 (C≡C), 284.25 (CO)	1680, 1682^{KBr}	468 (M^+, 100),[g] 440 ($M^+ - CO$, 19)
4	4.40 (Cp), 1.48 (CH_3), 5.39 (CH_2)	84.46 (Cp), 9.25 (C_5Me_5), 94.71 (C_5Me_5), 80.69(CH_2), 154.86 (C≡C), 287.07 (CO)	1663, 1663^{KBr}	538 (M^+, 100), 510 ($M^+ - CO$, 13)
5	4.64 (Cp), 4.76 (CH_2), 3.36 (OCH_3)	85.51 (Cp), 82.50 (CH_2), 58.75 (OCH_3), 156.97 (C≡C), 281.72 (CO)	1679, 1664^{KBr}	514 (M^+, 100), 486 ($M^+ - CO$, 11)

[a] C_6D_6 (7.15 ppm); d = doublet, t = triplet. [b] CD_2Cl_2, unless otherwise indicated. [c] Carbonyl stretch in methylene chloride, unless otherwise indicated. [d] EI; ion mass peaks with significant relative intensities (in parentheses) which correspond to assignable mass fragments or molecular ions are given. [e] Spectrum acquired in acetone-d_6. [f] The carbonyl ^{13}C NMR resonance for **1** was not observed due to limited solubility. [g] Exact molecular weight for **3**, calcd for $Co_3C_{20}H_{19}O_2$ 467.9381; obsd 467.9396.

to the formation of bis(carbyne) complexes[9] of the form $(CpCo)_3(\mu_3\text{-}CR)_2$. In the case of the 1,4-dihydroxy-2-butyne complex **1**,[10] however, an altogether different product is observed. In refluxing decalin (4 h), intramolecular dehydration and cyclization of the alkyne ligand proceeds smoothly to form a furyne ligand which is complexed to the Cp_3Co_3 skeleton.

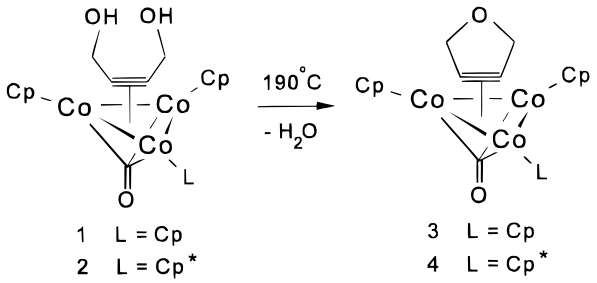

The furyne complex is also formed from **1** in refluxing isoquinoline (bp = 242 °C), but no reaction is observed in refluxing toluene, pyridine, or acetic acid. Thus, it appears that the formal dehydration reaction does not benefit from the presence of a mild acid or base and requires temperatures in excess of 120 °C. The presence of a strong acid (HBF_4) and lower temperatures (refluxing diethyl ether) leads, via decomposition of the alkyne complex, to intractable materials. The relatively mild conditions required for the dehydration and cyclization of this organic fragment indicate that the tricobalt cluster plays a significant role in the reaction beyond perturbing the alkyne toward a geometry favorable to cyclization. It is also significant that none of the bis(carbyne) complex is formed from the butynediol complex **1** in refluxing decalin. Under these conditions, most other alkyne complexes of this type undergo 15−30% conversion to bis(carbyne) complexes.[11] The dimethoxybutyne complex $(CpCo)_3(CO)(CH_3OCH_2C{\equiv}CCH_2OCH_3)$, **5**, also does not undergo alkyne scission in refluxing decalin (4 h) and is recovered in good yield.

Prolonged heating (24 h) of the butynediol complex **1** or the isolated furyne complex **3** results in partial decomposition of the cluster and the formation of the tetranuclear furyne complex $(CpCo)_4(\mu_4\text{-}\eta^2\text{-}\overline{CH_2C{\equiv}CCH_2O})$ in low yield.[8] No tetranuclear furyne complex of any type is isolated upon prolonged heating of the Cp* containing complexes **2** and **4**.

The furyne complex **3** is much more resistant to CO-induced fragmentation than the diphenylacetylene complex $(CpCo)_3(CO)(PhC{\equiv}CPh)$, **6**.[11] Heating a decalin solution of **3** to 200 °C for 4 h in a sealed tube containing an atmosphere of carbon monoxide does not result in significant fragmentation. Similar experiments performed with **6** give rise to greater than 70% fragmentation to form $CpCo(CO)_2$, diphenylacetylene, and other unidentified products.[12]

In the region of the parent ions, the mass spectra of $(CpCo)_3(CO)(RC{\equiv}CR)$ alkyne complexes typically show prominent ion mass signals consistent with the loss of the carbonyl ligand.[13] In contrast to this, the butynediol complexes **1** and **2** show prominent mass signals consistent with the loss of H_2O (Table 1) and formation of the furyne ligand. The mass spectrum of the monoadduct complex of 2,4-hexadiyne-1,6-diol $(CpCo)_3(CO)(HOCH_2C{\equiv}CC{\equiv}CCH_2OH)$,[10] however, does not exhibit a mass signal consistent with dehydration. Interestingly, ion mass signals indicative of the loss of CO are observed in the mass spectra of the furyne complexes **3** and **4** and the dimethoxybutyne complex **5**, although these complexes do not undergo alkyne scission in solution. Consistent with the above observations, the furyne complex **3** is also formed by heating a film of the butynediol complex in an NMR tube at 220 °C for 30 min. Yields in this presumed solid state reaction are lower than those observed in refluxing decalin.

Comparison of the infrared spectra of the all-Cp containing complexes **1** and **3** to the spectra of the Cp* containing complexes **2** and **4** reveals that the substitution of a Cp* ligand for a Cp ligand results in the predictable lowering of the CO stretching frequency (Table 1). The carbonyl stretches in the solution spectra of **2** and **4** are shifted to lower energy by 16 and 17 cm^{-1} relative to **1** and **3**, respectively. These shifts are consistent with an increase in the electron density at the metals due to the presence of the Cp* ligands in **2** and **4**, resulting in greater back-bonding to the π^* orbitals of the carbonyl ligands. The solution carbonyl stretching frequency of **3** is similar to the stretching frequency observed for the noncyclic analogue, the dimethoxybutyne complex **5**. The carbonyl stretching

(10) Barnes, C. E.; Orvis, J. A.; Finniss, G. M. *Organometallics* **1990**, *9*, 1695.
(11) Barnes, C. E.; King, W. D.; Orvis, J. A. Manuscript in preparation
(12) Orvis, J. A. Ph.D. Thesis, University of Tennessee, 1993.
(13) Freeman, M. B.; Hall, L. W.; Sneddon, L. G. *Inorg. Chem.* **1980**, *19*, 1132.

Table 2. Summary of Crystallographic Data for 3 and 4

	3	4
formula	$C_{20}H_{19}Co_3O_2$	$C_{25}H_{29}Co_3O_2$
mol wt	468.1	538.3
color; habit	black; diamond	black; rectangular
cryst syst	monoclinic	monoclinic
space group	$P2_1/c$	$P2_1/c$
a, Å	9.138(2)	16.673(3)
b, Å	23.327(6)	9.118(2)
c, Å	8.835(2)	14.549(3)
B, Å	117.23(2)	104.22(2)
V, Å^3	1674.7(7)	2144.0(8)
Z	4	4
D_{calcd}, g cm^{-3}	1.857	1.668
cryst size, mm	1.1 × 0.7 × 0.1	0.4 × 0.3 × 0.2
μ, (Mo Kα) cm^{-1}	294.5	23.11
T, K	173	173
abs corr	semi-empir. laminar	semi-empir.
parameters	227	272
λ (Mo Kα)	0.710 73	0.710 73
2θ limits	3.5−50.0	3.5−45.0
index ranges (hkl)	+9,+28,±10	+17,+11,±19
no. rflns collected	3466	3350
no. independent rflns	2959	2819
obsd rflns with $F > 4\sigma(F)$	2445	2334
R, %	4.82	4.39
wR, %	6.15	3.68
GOF	1.76	1.96

Table 3. Selected Bond Lengths (Å) and Bond Angles (deg) for 3 and 4

	3	4
Bond Lengths		
Co(1)−Co(2)	2.437(1)	2.467(1)
Co(2)−Co(3)	2.461(1)	2.449(1)
Co(3)−Co(1)	2.561(1)	2.529(1)
Co(1)−C(2)	1.869(5)	1.872(5)
Co(2)−C(2)	2.005(5)	2.005(5)
Co(2)−C(3)	1.982(6)	2.002(6)
Co(3)−C(3)	1.870(5)	1.877(5)
Co(1)−C(5)	1.930(7)	1.903(6)
Co(2)−C(5)	2.051(5)	2.034(5)
Co(3)−C(5)	1.927(7)	1.916(6)
C(5)−O(2)	1.187(8)	1.208(7)
C(1)−O(1)	1.453(8)	1.444(6)
C(1)−C(2)	1.495(8)	1.504(7)
C(2)−C(3)	1.374(9)	1.378(7)
C(3)−C(4)	1.505(8)	1.500(8)
C(4)−O(1)	1.464(8)	1.457(7)
Bond Angles		
Co(1)−Co(2)−Co(3)	63.0(1)	61.9(1)
Co(2)−Co(3)−Co(1)	58.0(1)	59.4(1)
Co(3)−Co(1)−Co(2)	58.9(1)	58.7(1)
C(1)−C(2)−C(3)	109.6(5)	109.4(4)
C(2)−C(3)−C(4)	109.4(5)	109.0(4)
O(1)−C(1)−C(2)	105.2(5)	104.8(4)
O(1)−C(4)−C(3)	104.5(5)	104.6(4)
C(1)−O(1)−C(4)	109.0(4)	109.2(4)

frequencies for all of the alkyne and cycloalkyne complexes **1**−**5** are consistent with triply-bridging carbonyl ligands.

^{1}H and ^{13}C NMR spectra for complexes **1**−**5** are typical of monocarbonyl Cp_3Co_3- and $Cp_2Co_2Cp^*Co$-based alkyne complexes.[10] At room temperature, single resonances are observed for both the cyclopentadienyl ligands and the methylene groups of **1**, **3**, and **5** in the proton and carbon NMR spectra. Room temperature proton spectra for **2** and **4** exhibit Cp and Cp* resonances, which integrate as 10 and 15 protons, respectively, as well as a methylene resonance which integrates as 4 protons. These observations imply that the alkyne ligands rotate freely above the tricobalt framework in solution, producing an apparent 3-fold molecular symmetry for these complexes. Similar observations have been reported for other cyclopentadienyl-based trinuclear alkyne complexes.[10,13,14]

Solid State Structures of 3 and 4. Single crystals of the furyne complexes **3** and **4** suitable for X-ray diffraction analysis were obtained by recrystallization from hexane/methylene chloride solvent mixtures, and the molecular structures of both complexes have been determined. Unit cell, data collection, and refinement parameters are summarized in Table 2, while selected bond lengths and angles are given in Table 3. The structure of **3** has been described briefly in an earlier communication.[8] Since these complexes are fluxional in solution at room temperature, the solid state structures should be viewed as limiting "canonical forms" which represent lowest energy structures resulting from the minimization of intramolecular interactions and solid state crystal packing forces. As shown in Figure 1, the structures of **3** and **4** are very similar. The μ_3-η^2 cycloalkyne ligand in each structure lies parallel to one metal−metal edge and the furyne ligand is tilted toward the opposite metal vertex (tilt angle from the normal to the metal plane: **3**, 18°; **4** 15°). In **4**, the furyne ligand is tilted toward the Cp*Co vertex of the metal triangle. The coordination geometry of the alkyne ligands in both complexes is best described as having the alkyne unit bridge all three metal atoms. The carbonyl ligand in each complex bridges all three metals in a μ_3-coordination geometry on the opposite side of the metal triangle from the furyne ligand. Both the alkyne and the carbonyl ligands are shifted toward the metal−metal edge which lies parallel to the alkyne. As shown in Figure 2, this shift is most pronounced for the carbonyl ligand. These structural features are consistent with the features observed in the structures of other $(CpM)_3(\mu_3\text{-CO})(RCCR)$ (M = Co, Rh) alkyne complexes described previously.[10,15]

The tilt and orientation of the cycloalkyne ligand in the structures of **3** and **4** are consistent with an η^2-|| bonding mode in which the alkyne may be considered σ-bonded to two cobalt atoms (M_1 and M_3) in the basal positions of a *nido*-M_3C_2 square pyramidal polyhedron (54 polyhedral skeletal bonding electrons) and π-bonded to the remaining metal vertex (M_2) in the apical position.[16] In **4**, both electronic and steric factors favor the

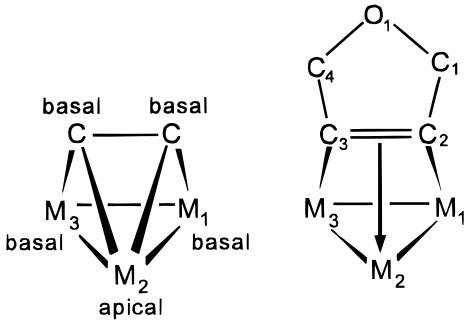

(14) Gardner, S. A.; Andrews, P. S.; Rausch, M. D. *Inorg. Chem.* **1973**, *12*, 2396.

(15) Trinh-Toan; Broach, R. W.; Gardner, S. A.; Rausch, M. D.; Dahl, L. F. *Inorg. Chem.* **1977**, *16*, 279.

(16) Thomas, M. G.; Muetterties, E. L.; Day, R. O.; Day, V. W. *J. Am. Chem. Soc.* **1976**, *98*, 4645.

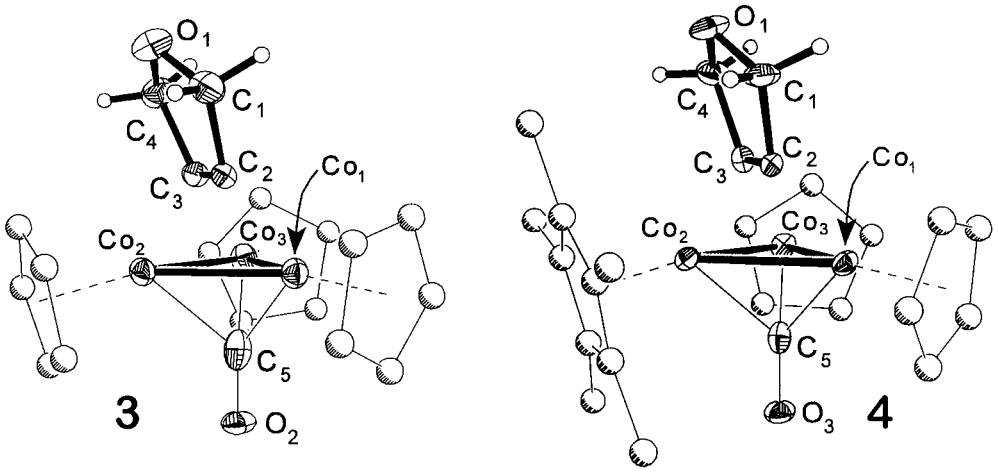

Figure 1. Molecular structures of the furyne complexes **3** and **4**.

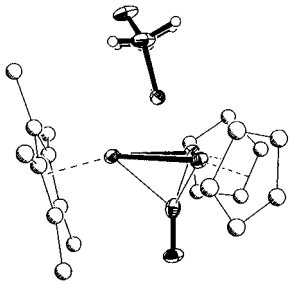

Figure 2. View of **4** showing the tilt and pucker of the furyne ligand and the positions of the furyne and carbonyl ligands relative to the Co_3 triangle.

location of the Cp* ligand in the apical position. In other *nido*-M_3C_2 systems, the alkyne has been shown to behave as an overall electron donor, bonding most strongly to the metals in the basal positions which are generally occupied by better electron-acceptor fragments.[17] In **4**, the metals with the better electron-acceptor capabilities are Co_1 and Co_3, which carry the Cp ligands. Steric interactions between the Cp* ligand and the furyne ligand in **4** also favor an alkyne orientation in which the furyne ligand occupies a position that is parallel to the Co_1-Co_3 edge. The shift in the positions of the alkyne and carbonyl ligands toward the metals in the basal positions in **3** and **4** reveals that back-donation of electron density into the empty π^* orbitals of these ligands is more pronounced for the basal metals.

The furyne ligands in both **3** and **4** are puckered, with the oxygen atom lying out of the plane of the four other atoms of the ring and tilted toward Co_2 (Figure 2). The puckering angles of the oxygen atoms from the $C_1-C_2-C_3-C_4$ plane in **3** and **4** are 15° and 17°, respectively. There is, however, no indication of any intra- or intermolecular bonding interaction between the furyne oxygen and the metals for either complex. The closest intramolecular $M-O_1$ distances are 3.56 Å for **3** and 3.60 Å for **4**, and all intermolecular $M-O_1$ distances are even larger for both complexes. The puckering of the furyne rings is presumably a result of solid state packing forces. The equivalence of the methylene protons in room temperature NMR spectra indicates either that the furyne rings are planar in solution or that ring inversion is fast and involves low barriers.

As the hybridization of the alkynes changes upon coordination to the metals, the alkyne bond lengths (C_2-C_3: **3**, 1.374(9) Å; **4**, 1.378(7) Å) increase to values between C−C double and C−C single bond lengths[18] and the bond angles (average of $C_1-C_2-C_3$ and $C_2-C_3-C_4$: **3**, 109.5°; **4**, 109.2°) decrease to values near that of a regular pentagon (108°). Comparison of the alkyne parameters in **3** and **4** to those of noncyclic trinuclear alkyne complexes reveals that the bond lengths fall within the normally observed range (1.30−1.45 Å) but that the C−C−R angles are considerably reduced (normal range 122−130°).[19] For example, the noncyclic 3-hexyne complex $(CpCo)_3(CO)(EtC{\equiv}CEt)$**,** **7**, exhibits an alkyne bond length of 1.370(5) Å but the alkyne bending angle is 127°.[10] Comparison of the alkyne parameters in **3** and **4** to those of the five-membered cycloalkyne in the structure of the zirconocene complex $Cp_2ZrP(CH_3)_3(C{\equiv}CCH_2CH_2\overline{CHCH_3})$ reveals that including a heteroatom in the ring and increasing the number of metal atoms with which the alkyne interacts results in a dramatic increase in the bond length and a small decrease in the bond angle of the alkyne. The alkyne bond length and average bond angle in the zirconocene complex are 1.296(6) Å and 112.8°, respectively.[3] The short alkyne bond distance observed for this complex has been attributed to decreased back-bonding into the π^* orbitals of the alkyne ligand.[20] The trend toward longer C−C bond lengths of coordinated alkynes as the number of interacting metal atoms increases has also been observed for noncyclic alkyne complexes.[19]

Comparison of the $M-C_{alkyne}$ bond distances observed for the furyne ligand in **3** to those of other $(CpCo)_3(CO)$(alkyne) complexes for which the solid state structures are known[10,21] reveals that the average distance in **3** is smaller than what has been observed in any other complex of this type. The average $M-C_{alkyne}$ bond distance for **3** of 1.932 Å is 0.023 Å shorter than the average of 1.955 Å observed for the diphenylacetylene complex **6**. Trends in the average distances observed

(17) (a) Halet, J. F.; Saillard, J. Y.; Lissillour, R.; McGlinchey, M.; Jaouen, G. *Inorg. Chem.* **1985**, *24*, 218. (b) Einstein, F. W. B.; Tyers, K. G.; Tracey, A. S.; Sutton, D. *Inorg. Chem.* **1986**, *25*, 1631.

(18) Representative values for C−C bond lengths: single C−C, 1.54 Å; double C=C, 1.34 Å; triple C≡C, 1.20 Å (Gordan, A. J.; Ford, R. A. *The Chemist's Companion*; Wiley: New York, 1972; p 109).

(19) Gervasio, G.; Rossetti, R.; Stanghellini, P. L. *Organometallics* **1985**, *4*, 1612.

(20) Chisholm, M. H.; Folting, K.; Huffman, J. C.; Lucas, E. A. *Organometallics* **1991**, *10*, 535.

(21) King, W. D. Ph.D. Thesis, University of Tennessee, Knoxville, TN, 1996.

for **6** and a number of other $(CpCo)_3(CO)$(alkyne) complexes with sterically less demanding alkyne substituent groups reveal that metal−alkyne bond distances in these complexes decrease with the steric bulk of the substituents.[21] Electronic effects resulting from cyclization of the alkyne ligand could also lead to shorter $M-C_{alkyne}$ bond distances. Decreasing the alkyne bond angle is expected to result in a lowering of the energy of the alkyne π^* orbitals.[22] Differences observed in ν_{CO} for some dinuclear carbonyl-based alkyne and cycloalkyne complexes have been attributed to enhanced metal−alkyne back-bonding in the cycloalkyne complexes resulting from the lowering of the energy of the π^* orbitals.[22] However, back-donation of electron density into these orbitals is also expected to lower the alkyne bond order. The alkyne bond length in the furyne complex **3** is identical within experimental uncertainties to that of the hexyne complex **7**, indicating that decreased steric interactions between the furyne ligand and the Cp_3Co_3 fragment lead to the shortening of the metal−alkyne bond lengths observed in the solid state structure of the furyne complex. The similarity of the ν_{CO} frequencies observed in the IR spectra of **3** and the dimethoxybutyne complex **5** also indicates that back-donation does not increase as a result of cyclization. The average metal−alkyne bond distance for **4** of 1.939 Å is similar to the average in **3**, indicating that back-donation into the alkyne π^* orbital does not increase due to the substitution of a Cp* ligand for a Cp ligand.

The metal−metal bond distances in the furyne complexes, **3** and **4**, fall into two groups: two shorter apical−basal metal−metal bonds (Co_2-Co_1 and Co_2-Co_3) and one longer basal−basal bond (Co_1-Co_3). All metal−metal distances are longer in **3** than those in the hexyne complex **7**, with the basal edge Co_1-Co_3 bond in **3** being particularly long (2.561(1) Å for **3** versus 2.480(1) Å for **7**). Differences in the metal−metal bonding in **3** and **7** are presumably associated with the reduced metal−alkyne bond distances observed for **3**. The substitution of a Cp* ligand for a Cp ligand at Co_2 in **4** results in increased metal−metal distances to Co_2 and a decrease in the Co_1-Co_3 bond distance compared to the all-Cp complex. These structural features may be explained by electronic or steric effects. The increased electron density at the Cp*Co vertex decreases metal−metal interactions and increases metal−metal bond distances to Co_2. As a consequence of this, metal−metal interactions along the structurally unique edge increase as Co_1 and Co_3 are rendered somewhat electron deficient. Steric interactions between Cp and Cp* ligands would have similar effects on the metal−metal bond lengths in **4**.

In both **3** and **4**, the Cp and Cp* ligands are oriented slightly below the metal plane. The effect is most pronounced for the unique Cp ligand in **3** and the Cp* ligand in **4**, since these are the vertices toward which the furyne ligand leans. The fact that steric interactions have increased in **4** is first evident in the observation that the furyne ligand does not lean as far toward Co_2 and that all Cp and Cp* ligands are pushed farther below the metal plane than in **3**. As was mentioned earlier, apical−basal bond lengths in **4** are increased relative to **3**. Olsen and Dahl have previously ascribed the metal−metal bond lengthening observed upon substituting Cp with Cp* ligands in similar trinuclear complexes to steric effects between adjacent Cp* ligands.[23] The structural features of **4** indicate that adjacent Cp* and Cp ligands also interact sterically. However, it is interesting to note that the Cp and Cp* ligands in **4** are not aligned head-to-tail, as has been observed for trinuclear complexes containing three mutually bound Cp*Co fragments.[24]

The structural differences observed for the carbonyl ligands in **3** and **4** are the result of an increase in electron density at all three metal atoms upon substitution of a Cp* ligand for a Cp ligand. An average decrease of 0.018 Å is observed in the metal−C_{CO} bond distances (average $M-C_5$ distance: **3**, 1.97 Å; **4**, 1.95 Å) as the degree of back-bonding to the carbonyl ligand increases in **4**. The carbonyl ligand retains a triply-bridging bonding mode in **4**, and there is no significant shift in the position of the ligand toward any given metal atom relative to the position of the carbonyl ligand in **3**. There is an increase of 0.021 Å in the C_5-O_2 bond length in **4** relative to the bond distance in **3**, consistent with the previously described shift in the carbonyl stretching frequency. Comparison of the changes observed in the bonding of the carbonyl ligand to the tricobalt core in **3** and **4** with the above observations in the metal−alkyne bonding in these complexes indicates that the increased electron density at the metals in **4** results in increased back-donation into the π^* orbital of the carbonyl ligand but not into the π^* orbital of the alkyne ligand.

Variable-Temperature NMR Studies. $(CpCo)_3(\mu_3$-CO)(RCCR) alkyne complexes typically show only a single cyclopentadienyl resonance in their ^1H and ^{13}C NMR spectra, even at low temperatures (~170 K).[21] The signals for the Cp ligands are equilibrated due to the rapid rotation of the alkyne ligand relative to the NMR time scale as described earlier. Variable-temperature ^1H NMR data for complexes **3**, **5**, **6**, and **7** show no changes in any resonances aside from slight temperature dependencies of their chemical shifts. Similar experiments performed on **4** gave quite different results. At 171 K, the methylene signals of the furyne ligand are observed as two doublets. These resonances broaden as the temperature is raised and coalesce at 195 K to a single resonance, which sharpens at room temperature (Figure 3). No broadening or coalescence behavior is observed in any other resonance of **4**. The coalescence phenomenon is consistent with the freezing out of the furyne ring in a position that is parallel to the edge containing the two CpCo vertices and similar to the structure observed in the solid state. This geometry renders the geminal methylene protons of the furyne ring nonequivalent, with one set pointing toward the Cp* ligand and the other pointing toward the $(CpCo)_2$ edge.

Figure 3 shows the experimental and simulated[25] NMR spectra for the coalescence of the methylene

(22) (a) Schilling, B. E. R.; Hoffman, R. *J. Am. Chem. Soc.* **1979**, *101*, 3456. (b) Hoffman, D.; Hoffman, R.; Fisel, R. *J. Am. Chem. Soc.* **1982**, *104*, 3858.

(23) Olson, W. L.; Dahl, L. F. *J. Am. Chem. Soc.* **1986**, *108*, 7657.

(24) Casey, P. C.; Widenhoeffer, R. A.; Hallenback, S. L.; Hayashi, R. K.; Powell, D. R.; Smith, G. W. *Organometallics* **1994**, *13*, 1521.

(25) Simulated line shapes were produced using the program DNMR5.[26]

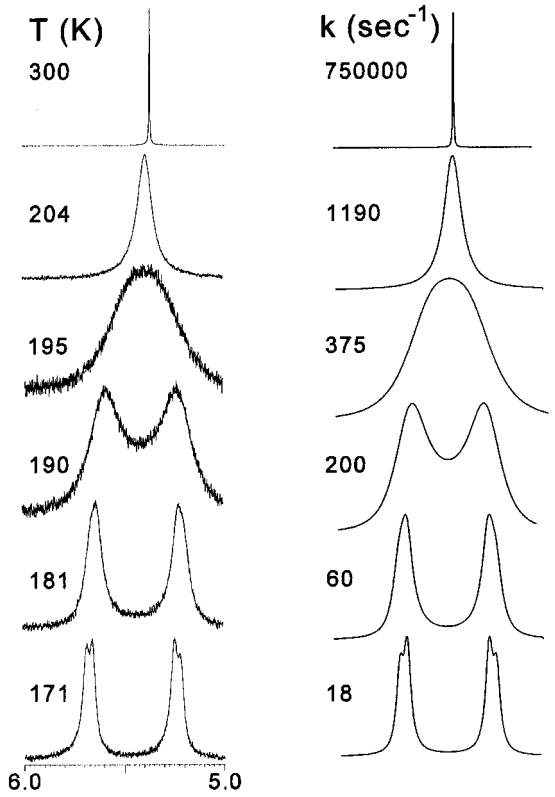

Figure 3. Experimental and simulated ^{1}H NMR spectra of the methylene signals of **4** in CD_2Cl_2. Rate constants for the motion of the furyne ring are given for each temperature.

signals observed for **4**. Total line shape analysis[26] of these signals as a function of temperature yields the activation parameters for the motion of the furyne ring: $\Delta G^{\ddagger}$ (300 K) = 39.4(2) kJ/mol, $\Delta S^{\ddagger} = -18(2)$ J/mol, and $\Delta H^{\ddagger} = 34.0(4)$ kJ/mol. Accurate modeling of the methylene resonances of **4** required a geminal coupling constant of 14.5 Hz and a separation of 0.447 ppm for the two methylene signals at the lowest temperature.

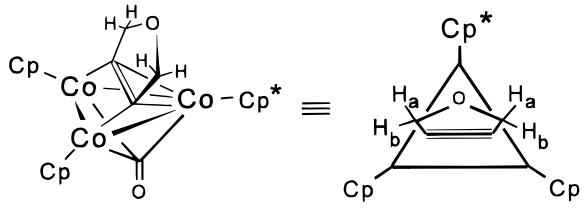

A second explanation exists for the coalescence behavior observed for the methylene resonances of **4**. Slowed ring inversion of a puckered furyne ring in solution at low temperatures (see discussion of the solid state structures) while maintaining fast rotation of this ligand relative to the tricobalt framework would lead to a similar coalescence behavior of these resonances. However, we have observed coalescence behavior for other noncyclic $(CpCo)_2(Cp^*Co)(CO)(RCCR)$ alkyne complexes that is consistent only with slowed alkyne rotation.[27] On the basis of these experiments and the fact that no coalescence is observed in the variable-temperature spectra of the all-Cp furyne complex **3**, we believe

(26) (a) Binsch, G.; Kessler, H. *Angew. Chem., Int. Ed. Engl.* **1980**, *19*, 411. (b) Wickenheiser, E. B.; Cullen, W. R. *Inorg. Chem.* **1990**, *29*, 4671.

(27) Försterling, F. H.; Barnes, C. E. Manuscript in preparation.

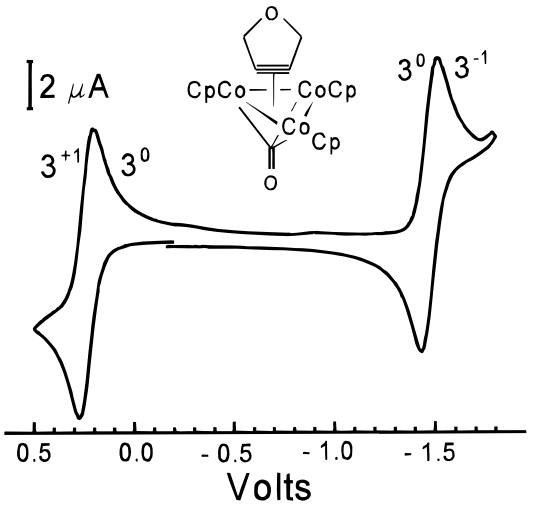

Figure 4. Cyclic voltammogram of **3** (1 mM in CH_2Cl_2, ν = 100 mV/s, Pt, 0.1 mM TBAP supporting electrolyte).

that slowed alkyne rotation is the source of the coalescence phenomenon observed in the methylene signals of **4**.

Electrochemistry. In an effort to evaluate the effects of cyclization of the alkyne ligand upon the electronic structure of the cluster, cyclic voltammetry (CV) experiments were performed on the $(CpCo)_3(CO)$-(furyne) complex, **3**. Figure 4 shows the cyclic voltammogram of a 1 mM solution of **3** obtained at a platinum electrode in a methylene chloride solution containing 0.1 M tetrabutylammonium hexafluorophosphate (TBAP) as the supporting electrolyte. Chemically and electrochemically reversible one-electron oxidative and reductive couples are observed at +0.235 and −1.466 V, respectively. Peak currents for both redox features show a linear dependence with $\nu^{1/2}$, and i_{pa}/i_{pc} ratios are near unity at scan rates ranging from 100 to 1000 mV/s. The separation of the anodic and cathodic peak potentials, ΔE_p, is near 80 mV for each of these couples, similar to the peak separation observed for the ferrocene/ferrocenium couple in this cell. A comparative CV study was conducted on the dimethoxybutyne complex $(CpCo)_3(CO)(CH_3OCH_2C{\equiv}CCH_2OCH_3)$, **5**, the noncyclic analogue of **3**. The cyclic voltammogram of **5** shows chemically and electrochemically reversible one-electron oxidative and reductive waves centered at +0.192 and −1.553 V, respectively. Thus, both the oxidative and reductive waves of the furyne complex are shifted to more positive potentials by ∼40 and ∼90 mV, respectively, relative to the same waves in the cyclic voltammogram of **5**. The similarity of the CVs for the furyne complex and the dimethoxybutyne complex indicates that cyclization of the alkyne unit in **3** does not lead to significant changes in the upper bonding levels of the Cp_3Co_3 core.

Summary and Conclusions

The structural, spectroscopic, and electrochemical properties of the all-Cp furyne complex **3** are similar to those of noncyclic analogues, indicating that ring formation does not result in large perturbations in the electronics of the Cp_3Co_3 core. The major structural

changes observed for **3** in the solid state are the reduction of the bond angle through the coordinated alkyne group due to cyclization, and a decrease in the metal−alkyne bond distance, which is attributed to decreased steric interactions between the alkyne and Cp_3Co_3 framework. The similarity of the $C-C_{alkyne}$ bond length in the solid state structure and the carbonyl stretching frequency in the infrared spectrum of **3** to the values observed for noncyclic analogues indicates that cyclization does not lead to increased metal−alkyne back-donation as has been observed for dinuclear carbonyl-based cycloalkyne complexes.[3] Similar $E_{1/2}$ values observed for the reversible one-electron oxidative and reductive couples in cyclic voltammograms of **3** and the dimethoxybutyne complex **5** further confirm that the differences in the electronic structures of the cyclic furyne complex and noncyclic analogues are small.

The furyne complexes **3** and **4** represent the first examples of cycloalkyne complexes coordinated to monocarbonyl Cp_3Co_3-type clusters. Comparative structural studies on these complexes reveal that the substitution of a Cp* ligand for a Cp ligand causes minor changes in the metal core, which can be attributed to electronic or steric effects. The observation that the position of the coordinated carbonyl ligand relative to the metal triangle does not change on going from **3** to **4** indicates that the increased electron density from the Cp* ligand is evenly distributed about the metals and points to steric factors as a significant contributor to the changes in metal−metal bonding interactions. Greater electron density at the metals in **4** results in a significant reduction in the average $M-C_{CO}$ bond distance, while the average $M-C_{alkyne}$ bond distance remains constant. These observations are consistent with a greater increase in back-donation to the carbonyl ligand than to the alkyne ligand. Spectroscopic studies on **4** indicate that the greater electron-donating ability of the Cp* ligand results in a lower CO bond order. Furthermore, steric interactions with the furyne and Cp* ligands increase the barrier to rotation of the furyne complex relative to the all-Cp furyne complex **3**.

Experimental Section

General Comments. 2-Butyne-1,4-diol, obtained from Aldrich, was recrystallized once before use. The tetrabutylammonium hexafluorophosphate (TBAP) supporting electrolyte was recrystallized three times from ethanol before use in the electrochemical experiments. All solvents were reagent grade and were distilled under dry N_2 from Na/K alloy (hexane, toluene, diethyl ether, tetrahydrofuran) or calcium hydride (methylene chloride). Air-sensitive complexes were handled in an inert atmosphere drybox (Innovative Technologies, MB-150) under a helium atmosphere or following standard Schlenk techniques using house nitrogen which was purified with a column of MnO on vermiculite followed by a column of activated 4 Å molecular sieves. Chromatographic separations (silica gel) were carried out under anaerobic and anhydrous conditions using flash chromatography columns. Nuclear magnetic resonance (NMR) spectra were acquired on a Bruker AMX400 Fourier transform instrument. Elemental analyses were performed by Desert Analytics-Organic Microanalysis of Tuscon, AZ.

Syntheses. $[Cp_2Fe][PF_6]$,[28] Cp_2Co,[29] $(CpCo)_3(CO)_2$,[30] and $(CpCo)_2(Cp^*Co)(CO)_2$[31] were prepared according to literature procedures. 1,4-dimethoxy-2-butyne was prepared from the reaction of butynediol with dimethyl sulfate following literature procedures.[32] $[Cp_2Co][PF_6]$ was prepared from cobaltocene and $[Cp_2Fe][PF_6]$ in a methylene chloride solution. The product precipitated from the solution upon the addition of hexane and was filtered from the solution as a bright yellow solid.

$(CpCo)_3(CO)(C_4H_6O_2)$, 1, and $(CpCo)_2(Cp^*Co)(CO)(C_4H_6O_2)$, 2. **1** was prepared by the reaction of $(CpCo)_3(CO)_2$ (780 mg, 1.82 mmol) with an excess of 2-butyne-1,4-diol (390 mg, 4.53 mmol) in a toluene solution (80 mL) saturated with the alkyne. After 30 min, the toluene solvent was removed under vacuum from the dark brown solution to give a brown residue of impure **1**. **2** was prepared in a similar manner by the reaction of butynediol with $(CpCo)_2(Cp^*Co)(CO)_2$. Approximately 50% of the starting reagents are lost in the syntheses of **1** and **2** due to the formation of the tricarbonyl complexes $(CpCo)_3(CO)_3$[33] and $(CpCo)_2(Cp^*Co)(CO)_3$, respectively. The alkyne complexes eluted from the columns as yellow-brown or orange-brown bands in tetrahydrofuran or tetrahydrofuran/ether after the elution of the tricarbonyl complexes in methylene chloride. Recrystallization of **1** and **2** from hexane/methylene chloride solutions gave black microcrystalline solids or brown powders. The isolated yield of microcrystalline **1** was 19% (165 mg, 0.339 mmol), based on $(CpCo)_3(CO)_2$. Similar yields were obtained for **2**. Anal. Calcd for **1** ($C_{20}H_{21}Co_3O_3$): C, 49.41; H, 4.35. Found: C, 48.71; H, 3.90. Anal. Calcd for **2** ($C_{25}H_{31}Co_3O_3$): C, 53.98; H, 5.62. Found: C, 54.24; H, 5.62.

$(CpCo)_3(CO)(C_6H_{10}O_2)$, 5. The dimethoxybutyne complex **5** was prepared from $(CpCo)_3(CO)_2$ and excess alkyne following the procedure described for **1**. After removal of the toluene solvent, the brown-black residue was dissolved in a minimal amount of methylene chloride and added to the column. The tricarbonyl complex was removed with methylene chloride, and the column was flushed with hexane. **5** eluted from the column with 50−100% ether in hexane as an orange-brown band and was recrystallized from a hexane/methylene chloride solution to give black needle crystals.

$(CpCo)_3(CO)(C_4H_4O)$, 3, and $(CpCo)_2(Cp^*Co)(CO)(C_4H_4O)$, 4. **3** (63 mg, 0.134 mmol) was prepared in 69% yield by heating 95 mg (0.195 mmol) of the butynediol complex **1** in refluxing decalin (bp 190 °C) for 4 h. After the solution was cooled, it was poured directly onto a column of silica and the translucent band of decalin was removed with several volumes of hexane. The reddish-brown furyne complex eluted in hexane/ether. The Cp* containing furyne complex **4** was prepared from **2** and isolated in a similar manner in approximately the same yield as for **3**. The furyne complexes were recrystallized from hexane/methylene chloride solutions to give black microcrystalline solids or brown powders. Anal. Calcd for **3** ($C_{20}H_{19}Co_3O_2$): C, 51.31; H, 4.09. Found: C, 51.02; H, 4.02. Anal. Calcd for **4** ($C_{25}H_{29}Co_3O_2$): C, 55.78; H, 5.43. Found: C, 56.13; H, 5.47.

Variable-Temperature NMR Spectra and Dynamic NMR Simulations. Variable-temperature NMR studies were performed in flame-sealed NMR tubes in CD_2Cl_2, which was dried over calcium hydride and vacuum transferred into the NMR tube. The temperature was calibrated to ±1 K following the procedures described by Van Geet.[34] For all of the variable-temperature spectra, a minimum of 15 min was allowed for temperature equilibration of the sample. NMR simulations were performed using the dynamic NMR fitting program DNMR5.[26] The geminal coupling constant used to

(28) Schumann, H. *J. Organomet. Chem.* **1986**, *304*, 341.
(29) Winkinson, G.; Cotton, F. A.; Birmingham, J. M. *J. Inorg. Nucl. Chem.* **1956**, *2*, 95.
(30) Barnes, C. E.; Orvis, J. A. *J. Am. Chem. Soc.* **1989**, *111*, 4992.
(31) (a) Barnes, C. E.; Dial, M. R. *Organometallics* **1988**, *7*, 782. (b) Barnes, C. E.; Dial, M. R.; Orvis, J. A.; Staley, D. L.; Rheingold, A. L. *Organometallics* **1990**, *9*, 1021.
(32) Brandsma, L. *Preparative Acetylenic Chemistry*; Elsevier Publishing Co.: 1971; p 172.
(33) (a) King, R. B. *Inorg. Chem.* **1966**, *5*, 2227. (b) Vollhardt, K. P. C.; Bercaw, J. E.; Bergman, R. G. *J. Organomet. Chem.* **1975**, *97*, 283.
(34) (a) Van Geet, A. L. *Anal. Chem.* **1968**, *40*, 2227. (b) *Ibid.* **1970**, *42*, 679.

model the methylene coalescence was 14.5 Hz, and the separation between the two methylene resonances was 178.8 Hz at the lowest temperature and 153.0 Hz at the highest temperature. Initial estimates of T_2 for the methylene protons were estimated from line widths of the Cp resonances and ranged from 0.03 s at the lowest temperature to 0.2 s. The error in the rate constant at the coalescence temperature is ±1%. Final simulated line shapes were obtained via an iterative parameter search involving the exchange constant k, T_2, and the chemical shift separation of the resonances. Full details of the fitting procedure may be found in the Supporting Information. The rate constants which accurately modeled the experimental spectra at each temperature are given in Figure 4. The activation parameters $\Delta H^{\ddagger}$ and $\Delta S^{\ddagger}$ were determined from the plot of $\ln(k/T)$ versus $1000/T$. Estimated standard deviations (σ) in the slope and y-intercept of the Eyring plot determined the error in $\Delta H^{\ddagger}$ and $\Delta S^{\ddagger}$, respectively. The standard deviation in $\Delta G^{\ddagger}$ was determined from the formula: $\sigma(\Delta G^{\ddagger})^2 = \sigma(\Delta H^{\ddagger})^2 + [T\sigma(\Delta S^{\ddagger})]^2 - 2T\sigma(\Delta H^{\ddagger})\sigma(\Delta S^{\ddagger})$.[26a]

Electrochemistry. Electrochemical investigations were performed on a BAS-100 Electrochemical Analyzer. All experiments were carried out at room temperature under anaerobic conditions using a specially designed vacuum electrochemical cell.[35] Degassed methylene chloride was vacuum-transferred into the three-electrode cell, which generally contained about a milligram of analyte and as little as 0.5 mL of solvent. A 0.1 M TBAP and 1−3 mM analyte solution was used. The working electrode was a platinum disk, the auxiliary electrode was platinum wire, and a Ag/AgCl pseudo reference electrode was used. All $E°$ values were referenced internally to the $0/1^+$ redox couple of $[Cp_2Co][PF_6]$ at −0.851 V. The ferrocene/ferrocenium couple is observed at +0.482 V in this cell.[36] The redox couples of ferrocene and cobaltocenium were used to define electrochemical reversibility. The one-electron nature of the redox couples for **3** and **5** was determined by the comparison of the ratio of peak current values (i_p) and the concentration (c) to the i_p/c ratio obtained for ferrocene. Positive feedback iR compensation was used to minimize the effects of solution resistance.

X-ray Structure Determination. Crystal data for **3** and **4** are collected in Table 2. Minimally air-sensitive reddish-brown crystals of **3** were prepared by slow evaporation of a hexane/methylene chloride solution in the drybox. Reddish-brown crystals of **4** were prepared by slow cooling of a hexane/methylene chloride solution. The crystals were lightly coated in oil (Paratone N from Exxon Chemical Americas), mounted on glass fibers, and then cooled to −100 °C in a nitrogen gas stream. Unit-cell parameters were determined through least-squares refinement of the angular settings for 47 reflections for **3** and 33 reflections for **4** ($5° \leq 2\theta \leq 35°$). Data were collected on a Siemens R3m/V diffractometer with a graphite monochromator (λ(Mo Kα) = 0.710 73 Å). A semi-empirical laminar absorption correction (six reflections, Ψ scans, 216 data) was applied to the data for **3**. An ellipsoidal absorption correction (six reflections, Ψ scans, 216 data) was applied to the data for **4**.

Solution and Structure Refinement. Initial solutions were obtained for both structures by direct methods, which located the metal atoms. Locations of the remaining non-hydrogen atoms were determined through subsequent difference Fourier analysis and least-squares refinement. All non-hydrogen atoms were refined anisotropically.

Structural solutions and least squares refinements were performed using the program SHELXTL PLUS Release 4.11/V provided by Siemens.

Figures 1 and 2 show the structures and numbering schemes, and Table 3 provides a list of pertinent bond angles and bond lengths for complexes **3** and **4**. All thermal ellipsoids are drawn at the 50% level. In order to simplify the figures, dotted lines are drawn from the metal atoms to the centroid of the Cp ligands and the bonds between the metal atoms and the alkyne units are omitted. Full structural details for **3** and **4** are provided in the Supporting Information.

Acknowledgment is made to the donors of the Petroleum Research Fund (PRF29106-AC5), administered by the ACS, for partial support of this research. We also thank Dr. Frank Holger Försterling for his assistance in the dynamic NMR line shape simulations.

Supporting Information Available: Text giving the protocol for the dynamic NMR line shape analysis for complex **4** and tables of complete structural determination, data collection and solution and refinement parameters, bond distances and angles, anisotropic displacement coefficients for all nonhydrogen atoms, hydrogen atom coordinates and isotropic displacement coefficients for both **3** and **4** (20 pages). Ordering information is given on any current masthead page.

OM960867Z

(35) Barnes, C. E.; King, W. D. Manuscript in preparation.
(36) Gritzner, G.; Kuta, J. *Pure Appl. Chem.* **1984**, *56*, 461.